SUPPLEMENTARY INFORMATION FOR

Catalytic function of ionic liquids in polyethylene terephthalate glycolysis by molecular dynamics simulations

Mohamed Ahmed Nosir[a] and Manuel Angel Ortuño*[a]

[a] Centro Singular de Investigación en Química Biolóxica e Materiais Moleculares (CIQUS), Universidade de Santiago de Compostela, 15782 Santiago de Compostela, Spain.

E-mail: manuelangel.ortuno@usc.es

Table of Contents

1. Additional computational details

Fig. S1 shows the structures and atomic labels of the four components employed in this study: the IL cation $[Ch]^+$,[1] the IL anion $[PO_4]^{3-}$,[2] EG,[3] and PET oligomers.[4]

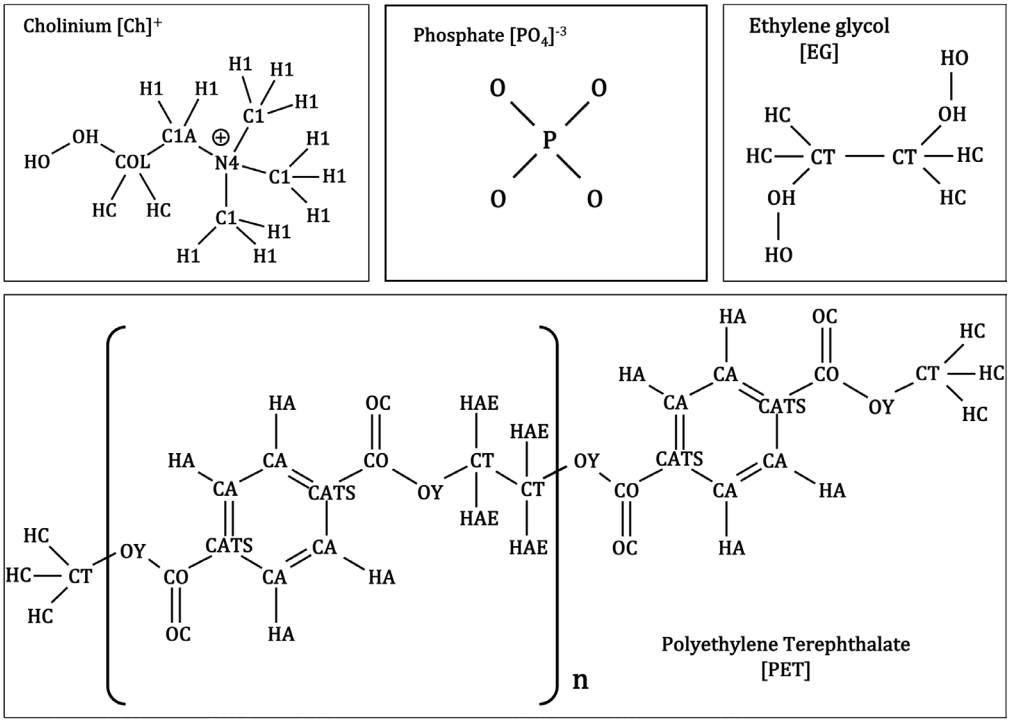

Fig. S1. Structures and force field nomenclature for the species under study.

Table S1 demonstrates that our simulations with the above-mentioned force fields are consistent with experimental and previously simulated densities as reported in literature.

Table S1. Comparison between experimental and simulated density values at 300 K for the systems under study.

Systems	Density ρ / g·cm^{-3}		
	This work	Experimental	Simulated
EG	1.10	1.11[5]	1.08[6]
PET	1.19	1.38[7]	1.22[8]
IL/EG	1.14	1.10[9]	n.a.
PET/EG	1.15	1.12[10]	n.a.
IL/PET	1.18	n.a.	n.a.
IL/PET/EG	1.16	1.18[11]	n.a.

2. PET···PET self-interaction

Fig. S2 collects the RDFs between the O of the carbonyl group of one PET dimer and selected H atoms from another PET dimer. These results suggest that there is a degree of aggregation between PET dimers. This is further confirmed by domain count analyses.

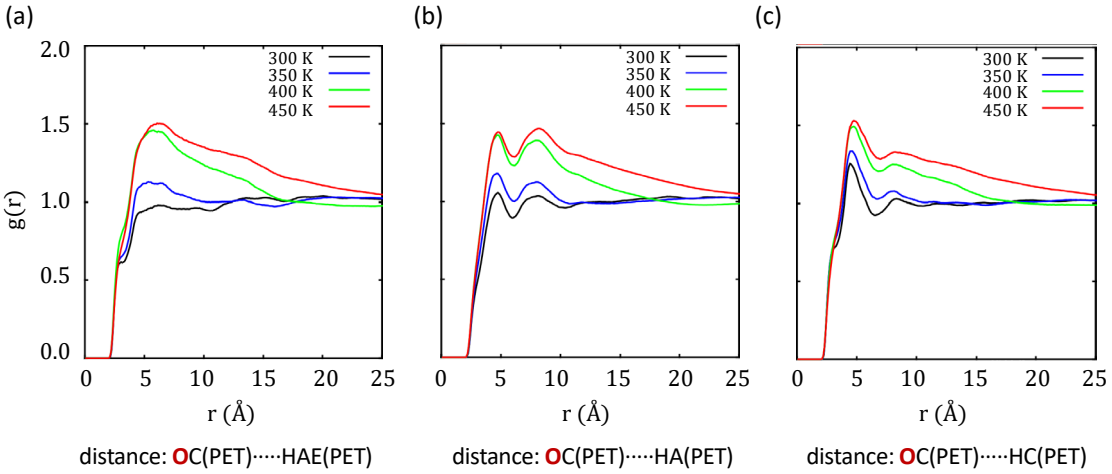

Fig. S2. Radial distribution functions (RDFs) between OC PET and (a) HAE, (b) HA, and (c) HC hydrogen atoms in PET for the ternary IL/PET/EG system at different temperatures. Refer to Fig. S1 for nomenclature.

3. Impact of oligomer length

In the main text, we model PET as a dimer. Here, we consider larger PET oligomers with 10, 25, and 100 units. The resulting interactions with EG (Fig. S3) and IL cation (Fig. S4) did not significantly change.

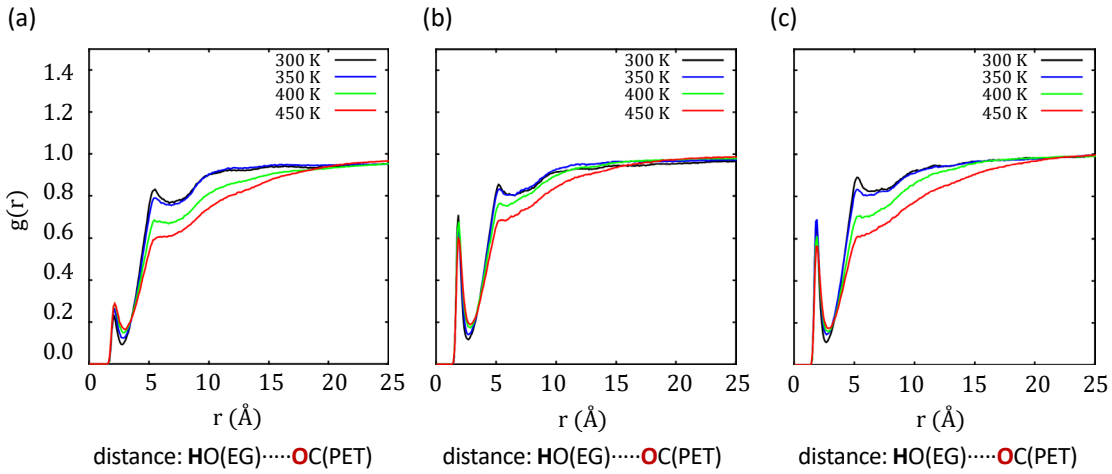

Fig. S3. Radial distribution functions (RDFs) between OC PET and OH in EG for the ternary IL/PET/EG system at different temperatures considering oligomer lengths of (a) 10, (b) 25, and (c) 100.

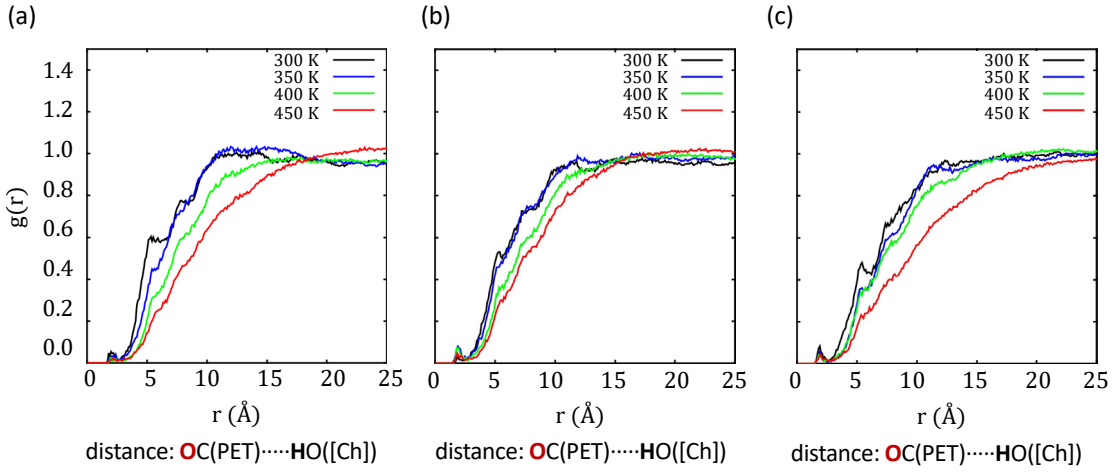

Fig. S4. Radial distribution functions (RDFs) between OC PET and OH in IL cation for the ternary IL/PET/EG system at different temperatures considering oligomer lengths of (a) 10, (b) 25, and (c) 100.

4. Impact of temperature on domain count

In the main text, we present the domain count at 450 K, the reaction temperature. For comparison, here we present the domain counts at 300 K (Table S2), 350 K (Table S3), and 400 K (Table S4).

Table S2. Domain count for each component in the ternary mixture IL/PET/EG and binary mixture IL/EG (in parenthesis) at 300 K.

	PET	EG	IL cation	IL anion
PET	1.0	1.0	2.6	94.5
EG	[a]	1.0 (1.0)	1.0 (1.0)	1.0 (1.0)
IL cation	[a]	[a]	190.0 (107.8)	128.9 (53.3)
IL anion	[a]	[a]	[a]	100 (100)

[a] The table is symmetric, so values are displayed only once.

Table S3. Domain count for each component in the ternary mixture IL/PET/EG and binary mixture IL/EG (in parenthesis) at 350 K.

	PET	EG	IL cation	IL anion
PET	1.0	1.0	2.8	99.5
EG	[a]	1.0 (1.0)	1.0 (1.0)	1.0 (1.0)
IL cation	[a]	[a]	135.4 (72.7)	76.7 (25.8)
IL anion	[a]	[a]	[a]	100 (100)

[a] The table is symmetric, so values are displayed only once.

Table S4. Domain count for each component in the ternary mixture IL/PET/EG and binary mixture IL/EG (in parenthesis) at 400 K.

	PET	EG	IL cation	IL anion
PET	1.9	1.0	9.9	99.5
EG	[a]	4.2 (1.0)	3.6 (1.0)	4.2 (1.0)
IL cation	[a]	[a]	101.6 (82.3)	50.3 (32.3)
IL anion	[a]	[a]	[a]	100 (100)

[a] The table is symmetric, so values are displayed only once.

5. Hydrogen bond lifetimes

The computed lifetimes[12] of selected hydrogen bonds in the IL/PET/EG system at different temperatures are shown in Table S5 .

Table S5. Mean value lifetimes (τ_{lf}) of selected hydrogen bonds in the ternary mixture IL/PET/EG at different temperatures.

Hydrogen bond	τ_{lf} / ps			
	T = 300 K	T = 350 K	T = 400 K	T = 450 K
O([PO_4]) · · · **H**O([Ch])	142.6	165.8	38.6	23.6
O([PO_4]) · · · **H**O(EG)	279.8	129.8	50.9	26.9
O([Ch]) · · · **H**O(EG)	167.3	73.9	40.6	19.4
O(EG) · · · **H**O(EG)	230.9	50.6	25.4	18.6
OC(PET) · · · **H**O(EG)	23.1	10.9	2.8	1.6
OC(PET) · · · **H**O([Ch]))	11.5	12.0	1.6	2.0

6. Cluster analysis

The results of the cluster analysis[13] are discussed as follows. Fig. S5a shows the cluster count function (CCF) which illustrates the distance at which connections between clusters are formed, based on a cutoff distance between them. At short cutoff distances, $[PO_4]^{3-}$, $[Ch]^+$, EG, and PET molecules are separated, resulting in a number of clusters equivalent to the number of individual components (CCFs are normalized by dividing by the number of molecules forming each binary interaction). As the cutoff distance increases, the number of clusters decreases, eventually approaching a single cluster of connected motifs. CCFs are consistent with RDFs, indicating that interactions for $[PO_4]^{3-}$, EG, and PET begin at a cutoff distance of *ca.* 1.7 Å, indicating H-bonds. Conversely, for PET and $[Ch]^+$ the cutoff distance is significantly larger, suggesting the presence of non-covalent electrostatic interactions. Fig. S5b displays the cluster distance distribution function (CDDF) which provides information about the probability of clustering based on the selected cutoff distance (CDDFs are normalized by dividing by the total number of molecules in the system). CDDFs identify different distances for different types of interactions and again align with RDFs.

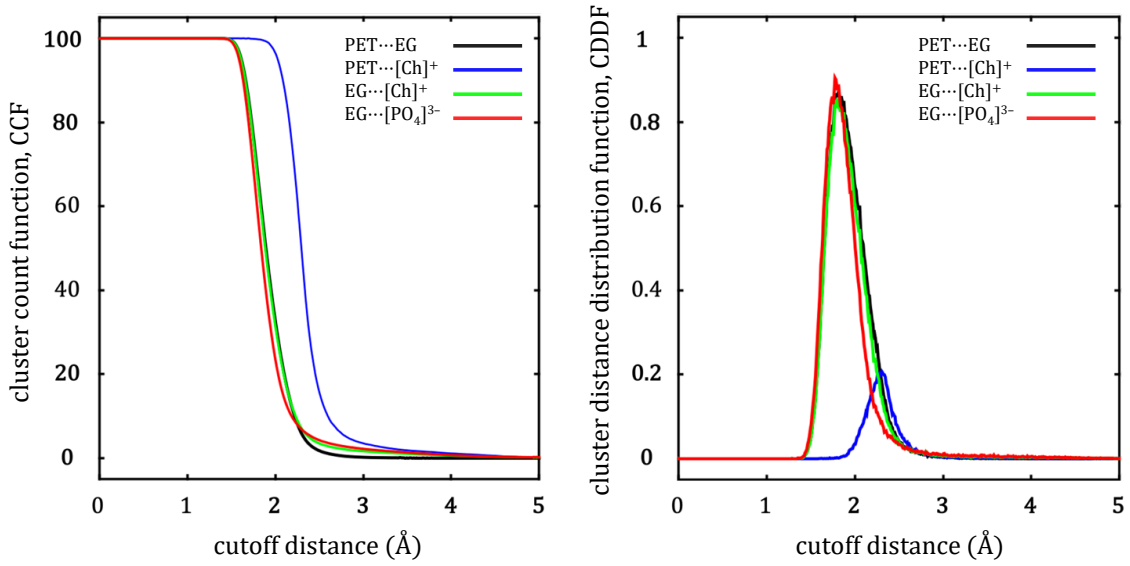

Fig. S5. Hierarchical clustering analysis showing (a) cluster count function and (b) cluster distance distribution function for the ternary mixture IL/PET/EG.

7. References

1 J. N. Canongia Lopes, J. Deschamps and A. A. H. Pádua, *J. Phys. Chem. B*, 2004, **108**, 2038.
2 R. Demichelis, N. A. Garcia, P. Raiteri, R. I. Malini, C. L. Freeman, J. H. Harding and J. D. Gale. *J. Phys. Chem. B*, 2018, **122**, 1471.
3 A. Kaiser, O. Ismailova, A. Koskela, S. E. Huber, M. Ritter, B. Cosenza, W. Benger, R. Nazmutdinov and M. Probst. *J. Molec. Liq.*, 2014, **189**, 20.
4 S. Jo, T. Kim, V. G. Iyer and W. Im. *J. Comput. Chem.*, 2008, **29**, 1859.
5 Y. Marcus, 2015. Ions in Solution and Their Solvation, 1st ed., Wiley.
6 O. Vital de Oliveira and L. C. Gomide Freitas, *J. Mol. Struct.*, 2005, **728**, 179.
7 D. Yang, H. Shi, L. Li, J. Li, K. Jabeen and P. Kolandhasamy, *Environ. Sci. Technol.*, 2015, **49**, 13622.
8 Q. Wang, D. J. Keffer, D. M. Nicholson and J. B. Thomas, *Macromolecules*, 2010, **43**, 10722.
9 R. B. Leron and M.-H. Li, *Thermochim. Acta*, 2012, **546**, 54.
10 M. J. O'Neil, The Merck index: an encyclopedia of chemicals, drugs, and biologicals; Royal Society of Chemistry, 2013.
11 M. Azeem, M. B. Fournet and O. A. Attallah, *Arab. J. Chem.*, 2022, **15**, 103903.
12 S. Gehrke and B. Kirchner, *J. Chem. Eng. Data*, 2020, **65**, 1146.
13 T. Frömbgen, J. Blasius, V. Alizadeh, A. Chaumont, M. Brehm and B. Kirchner, *J. Chem. Inf. Model.*, 2022, **62**, 5634.